Development 113, 825-839 (1991)
Printed in Great Britain © The Company of Biologists Limited 1991

Cell death in normal and rough eye mutants of *Drosophila*

TANYA WOLFF and DONALD F. READY

Department of Biological Sciences, Purdue University, West Lafayette, Indiana 47906, USA

Summary

The regular, reiterated cellular pattern of the *Drosophila* compound eye makes it a sensitive amplifier of defects in cell death. Quantitative and histological methods reveal a phase of cell death between 35 and 50 h of development which removes between 2 and 3 surplus cells per ommatidium. The timing of this epoch is consistent with cell death as the last fate to be specified in the progressive sequence of cell fates that build the ommatidium. An ultrastructural survey of cell death suggests dying cells in the fly eye have similarities as well as differences with standard descriptions of programmed cell death.

A failure of cell death to remove surplus cells disorganizes the retinal lattice. A screen of rough eye mutants identifies two genes, *roughest* and *echinus*, required for the normal elimination of cells from the retinal epithelium.

The use of an enhancer trap as a cell lineage marker shows that the cone cells, like other retinal cells, are not clonally related to each other or to their neighbors.

Key words: cell death, eye mutant, *Drosophila*, pattern formation, cell lineage.

Introduction

Cell death effects a host of developmental operations in virtually all metazoans, from the wholesale removal of tissues, to the cell-by-cell elimination of neurons making redundant or inappropriate connections in the nervous system. An initial overproliferation of cells followed by the elimination of surplus cells appears to be a common strategy when complex patterns, such as neural connectivity, must be imposed on populations of cells whose numbers cannot be precisely specified by the genome. Only the broadest outlines of the mechanism or mechanisms of cell death are known.

The *Drosophila* compound eye is a useful system for a mutational analysis of cell death. Its geometrically regular hexagonal array of unit eyes, or ommatidia, is achieved as approximately 1500–2000 surplus cells are eliminated by cell death in the retinal epithelium (Cagan and Ready, 1989*b*). At the close of pattern formation, near the end of the first third of pupal life, the fruit fly retina has an exact cellular order; each of the eight photoreceptors and dozen accessory cells that make up an ommatidium occupies a precise location in an extended cellular lattice. This makes the eye a sensitive detector of mutations that prevent normal cell death: surplus cells disrupt the smooth lattice and roughen the ommatidial array, a phenotype that can be easily selected.

This paper describes cell death in normal eye development and in two mutants with abnormal cell death. In normal eyes, quantitative and histochemical observations reveal a burst of cell death at the final phase of pattern formation. A detailed ultrastructural investigation of cell death in the *Drosophila* eye shows similarities to standard descriptions of programmed cell death (Bowen and Lockshin, 1981; Bowen and Bowen, 1990), as well as significant differences. Two mutants, *roughest* and *echinus*, selected in a screen of rough eye mutants, have a surplus of cells resulting from a decreased number of cell deaths in the eye. Further analysis of these and related mutants may provide insights into the mechanisms of cell death.

Materials and methods

Staging pupae

Stocks were raised at 20°C on a standard cornmeal agar food and maintained under constant illumination. White prepupae were collected and maintained for the reported interval. Time zero is the white prepupal stage. Canton S was used as the wild-type strain.

Somatic recombination

WG1296 was obtained from the Bloomington *Drosophila* stock center, Bloomington, Indiana. WG1296 contains a P-lArB (Bellen, 1989) insertion near 3D (personal communication, N. Swaminathan and E. Rulifson). *white* Oregon-R, WG1296 heterozygotes were irradiated to generate the wild type mosaics; Canton S/*y w* rst^{CT} heterozygotes were irradiated for the rst^{CT} mosaics. Larvae were irradiated with 900 rads using a ^{60}Co source 4 days after the parents were mated. Eyes were dissected in Ringer's solution at 65 h and fixed in 4% formaldehyde in PBS for a minimum of 30 min. Following a 30 min rinse in PBS-T (PBS with 0.3% Triton X-100), tissue was incubated overnight in anti-β-galactosidase monoclonal antibody (Promega, mouse IgG) at a dilution of

1:500. The Vector 'Elite' ABC kit was used to detect the primary antibody. Eyes were mounted in glycerol and viewed as whole mounts.

Cobalt sulfide stain

Cobalt sulfide staining (Melamed and Trujillo-Cenoz, 1975) was used to visualize both apical and basal surfaces of the retina. Eyes were dissected in Ringer's saline and then transferred to 2.5% glutaraldehyde in Ringer's for 10 min. The tissue was washed for several seconds in distilled water before being transferred into 2% $Co(NO_3)_2$ for 10–15 min. Tissue was then counterstained in 4% $(NH_4)_2S$ for 10 s. After a rinse in distilled water, eyes were removed from the lamina and mounted in glycerol.

Lead sulfide stain

A modified version of Locke and Huie's (1981) lead sulfide stain was used to visualize the apical surface of the retina. Eyes were dissected in Ringer's and transferred to primary fixative for 1–2 h at 4°C, then transferred to secondary fix and left overnight at 4°C. Tissue was taken through a series of washes beginning with 0.2 M sodium cacodylate buffer, pH 7.4 at room temperature, 0.1 M sodium cacodylate buffer, pH 5.6 and stock aspartate, pH 5.4. After the final rinse, eyes were transferred to lead staining solution for 5 min then replaced with fresh lead staining solution and incubated for an additional 5 h at room temperature. Tissue was washed in stock aspartate buffer and taken through two final washes of 0.1 M cacodylate, pH 5.4, before counterstaining in 8% $(NH_4)_2S$ for 5–10 s. Eyes were mounted in glycerol.

Cell counts

Cells included within a target area, defined by a central ommatidium and its 6 nearest neighbors, were counted at 5 h intervals between 30 and 60 h of pupal life. Cells straddling the target boundary were counted as one half of a cell. Eight target areas in each of six eyes were counted, totaling over 20 000 cells counted for each strain of flies investigated. The full complement of cone cells and primary pigment cells from the central ommatidium in addition to half this number for each of the six surrounding facets were included in the counts. Since photoreceptor assembly is complete at the earliest stages at which counts were taken, this group of cells was not included in the counts.

An Analysis of Variance (ANOVA) was used to assess the effect of mutation and developmental time on these cell counts. The three fly types, wild type, *ec* and rst^{CT}, were compared across 7 time points: 30, 35, 40, 45, 50, 55 and 60 h. These data are presented in Fig. 6. The ANOVA revealed significant main effects of both fly type and developmental time, $F(2105)=11.37$, $P<0.001$ and $F(6105)=31.47$, $P<0.001$, respectively. A Newman-Keuls post hoc analysis of fly type indicates that both *ec* and rst^{CT} contain a significant excess of cells as compared to wild type ($P<0.05$). Likewise the post hoc analysis of developmental age indicates that the number of cells decreased as development progressed for all fly types ($P<0.05$). The Newman-Keuls analysis of fly type by developmental age interaction, however, indicated that the decrease in cell numbers across development was greater for wild type. The mutants are characterized by a significant excess of cells during hours 50 through 60, rst^{CT} has significantly more cells than *ec* ($P<0.05$) which has significantly more cells than wild type. At 45 h *rst* has significantly more cells than either *ec* or wild type ($P<0.05$). Further, we can conclude that the pattern of cell elimination in both mutants does not deviate significantly from wild type in the earliest stages of cell die-off (i.e. 35 to 40 h after white pre-pupa) and that the stage that marks completion of cell removal coincides in all three strains examined, as shown by cell counts and AO staining.

Mutant screen

In addition to rst^{CT} and *ec* the following rough eye mutants were screened: *roughened eye* (*roe*), 3-47.6; *pebbled* (*peb*), 1-7.3; *lozenge* (*lz*) 1-27.7, *scabrous* (*sca*), 2-66.7; *uneven* (*un*), 1-54.4; *bulge bumpy* (bul^{bp}); *roughex* (*rux*), 1-15.0; *rugose* (*rg*), 1-11.0; and *facet-strawberry* (fa^{swb}) 1–3.0 (Lindsley and Grell, 1968). The rough eye phenotypes of these mutants do not appear to be related to a failure of cell death.

Anti-ubiquitin antibodies

40, 45 and 60 h eyes were fixed in 5% formaldehyde in PBS for a minimum of 45 min. After a 30 min rinse (3×10 min) in PBS-T, tissue was incubated overnight at 4° with either a rabbit polyclonal anti-ubiquitin antibody (Muller *et al.* 1988) or mouse monoclonal antibodies (kindly supplied by Dr V. Fried). The Vector 'Elite' kit or fluorescein avidin D (FITC from Vector), diluted 1:250 in PBS-T with 5% horse serum, were used as secondary antibodies.

Acid phosphatase

Acid phosphatase activity was assayed using protocols of Bowen and Ryder (1974) and *p*-nitrophenyl phosphate as a substrate. 40 and 70 h eyes were stained and prepared for light and electron microscopy.

Acridine orange

Acridine orange was used to identify late stage dying cells. The method used is after Spreij (1971). Briefly, animals were dissected in acridine orange in Ringer's (1.6×10^{-6}) and examined immediately using fluorescein filters.

Feulgen stain

Feulgen stain (Chayen *et al.* 1969) was used to visualize pycnotic nuclei in third instar eye discs.

Bromodeoxyuridine incorporation and visualization

BUdR labeling and scoring was performed as in Wolff and Ready (1991).

Electron microscopy

Tissue was fixed according to Baumann and Walz (1989) and embedded in Epon–Araldite. Material was serially sectioned on a Reichert microtome and mounted on Formvar-coated grids. A Philips 301 transmission electron microscope was used to view the sections.

Phalloidin staining

A rhodamine conjugate of phalloidin (Sigma) was used to stain wild type and rst^{CT} eyes at 45, 50, 55, 60 and 70 h of pupal development. Fragments of dying cells can be seen with phalloidin and was useful in assessing the presence of dead cells. Tissue was fixed for 15 min in 4% formaldehyde then stained overnight at 4° in 5% rhodamine–phalloidin, 5% horse serum, and 0.3% Triton X-100 in PBS. Tissue was carried through three 10 min changes of PBS-T and examined on a Biorad MRC-500 confocal microscope.

Results

The precise cellular organization of the *Drosophila*

compound eye is complete 65 h after the beginning of pupal life (Cagan and Ready, 1989*b*). The remaining two thirds of retinal development is devoted to the elaboration of specialized structures such as the lenses, rhabdomeres, and the pigments that give the eye its distinct red color. During this phase the eye also deepens from approximately 20 μm to 100 μm. These changes introduce considerable complexity into the eye and reconstruction of cell patterns in the adult eye usually requires tedious histology.

Cell patterns can be read in mid-pupal eye whole mounts with the same or better resolution than is possible in sections of the adult eye. These whole mounts can be viewed in their entirety, while the curvature of the adult eye permits a detailed reading of only those ommatidia cut reasonably tangentially. A schematic 65 h pupal ommatidium is shown in Fig. 1.

Cone cells are not clonally derived

Mosaic studies have shown that the photoreceptors and pigment cells of the compound eye are not specified by cell lineage (Ready *et al.* 1976; Lawrence and Green, 1979). The lens-secreting cone cells, however, have proved refractory to clonal analysis. Although cone cells contain the ommochrome pigments used to score cell genotypes in earlier work, the pigment granules are confined to small basal processes which are difficult to read in sectioned eyes. Enhancer traps, stably incorporated transgenes typically including *E. coli lac-Z* (O'Kane and Gehring, 1987; Bellen *et al.* 1989; Bier *et al.* 1989), offer a useful alternative genotype marker in mosaic studies (Blair, 1991).

A clonal analysis of the cone cells is possible with WG1296, an enhancer trap line which expresses *E. coli* β-galactosidase in the nuclei of all retinal cells, including cone cells. Clones of cells lacking the marker can be induced using somatic recombination, and easily detected in pupal eye whole mounts using anti-β-galactosidase immunohistochemistry. Cell identities in these eyes can be read unambiguously, given the stereotyped size, shape and position of retinal nuclei. In mosaic eyes, a clonal boundary can separate cone cells from each other and from neighboring cells in an apparently arbitrary fashion (Fig. 2). The cone cell quartet is not a clone, nor is a cone cell obligatorily the sister of a given adjacent cell. The equatorial cone cell and R7, for example, need not share a common mother cell. The non-clonal origin of ommatidia is evident in Fig. 3, which shows a complete β-galactosidase null clone.

Enhancer trap mosaics support a clonal origin for the mechanosensory bristles of the eye. Along the edge of a clone, the four cells of a bristle complex are either all *lacZ* negative or positive. This absence of mosaic bristles is consistent with mitotic labeling results in the eye, which indicate a single mother cell generates the bristle group (Cagan and Ready, 1989*b*).

Cell death eliminates two to three cells per ommatidium between 35 and 50 h after pupation

The external regularity of the adult ommatidial array is the product of a precise, underlying cellular lattice (Fig. 4A). The organization of this pattern begins along the morphogenetic furrow, the leading edge of a patterning wave that sweeps across the eye disc during the third instar. Once ommatidia are initiated at spaced intervals, they grow by accretion as undetermined neighbors are recruited into specific cell fates. This process continues locally, gathering cells around a single ommatidial rudiment until about 30 h of pupal life. By this time, the 8 photoreceptors, 4 cone cells and 2 primary pigment cells have grouped into stereotyped units, seen clearly on the apical surface of cobalt or lead sulfide stained eyes (Fig. 5, CS 30). Surrounding each unit is a population of unpatterned and undifferentiated cells. This population of interommatidial cells contains two to three more cells per ommatidium than can be accommodated in the final pigment cell mesh.

A phase of widespread cell death between 35 and 55 h of pupal life resolves the final form of the retinal lattice by eliminating approximately one third of the interommatidial cell population (Fig. 5, CS 30, 40, 50 and 60). By 35 h into pupation (not shown), the primary pigment cells have achieved their final positions, and over the next 5 h the bristles assume their characteristic locations. By 40 h the secondary and tertiary pigment cells are the only elements of the pattern that have not been sorted into their appropriate niches; the putative secondary pigment cells are frequently doubled end-to-end (Fig. 5, CS 40, asters) and at a vertex two to three cells (Fig. 5, CS 40, asterisks) can occupy the site of a future tertiary pigment cell. The final cellular tiling of the eye is achieved by 55 h (not shown). Between 55 and 60 h, the continuing expansion of the primary pigment cells reduces the apical outlines of the secondary and tertiary pigment cells to slender profiles.

The monolayer organization of the retinal epithelium permits a quantitative measurement of cell death (Fig. 6). All living cells, with the exception of the eight photoreceptors, can be accounted for on the apical surface of the eye. Eye whole mounts were stained using cobalt or lead sulfide and the apical profiles of cells were viewed using video microscopy. Cells were counted within a target area defined by a central ommatidium and its six nearest neighbors (Fig. 5, CS 60). Counts were made at 5 h intervals between 30 and 60 h of pupal life. Each point in Fig. 6 represents an average of 48 target areas, the sum of eight targets in each of six eyes. Each curve represents approximately 20 000 cells.

Cell counts show dying cells disappear from the apical surface between 35 and 55 h of pupal development (Fig. 6). The most rapid loss occurs between 35–40 h and counts level off by 55 h, the time at which the adult pattern of cells has been achieved. The absence of error bars at 60 h in wild type reflects the precision of the lattice. The noisiest component of the pattern is the secondary pigment cells, which are duplicated end-to-end with a frequency below 2.5 %. Abnormal numbers of cone cells and primary pigment cells are found in 1 % and 0.4 % of all ommatidia, respectively.

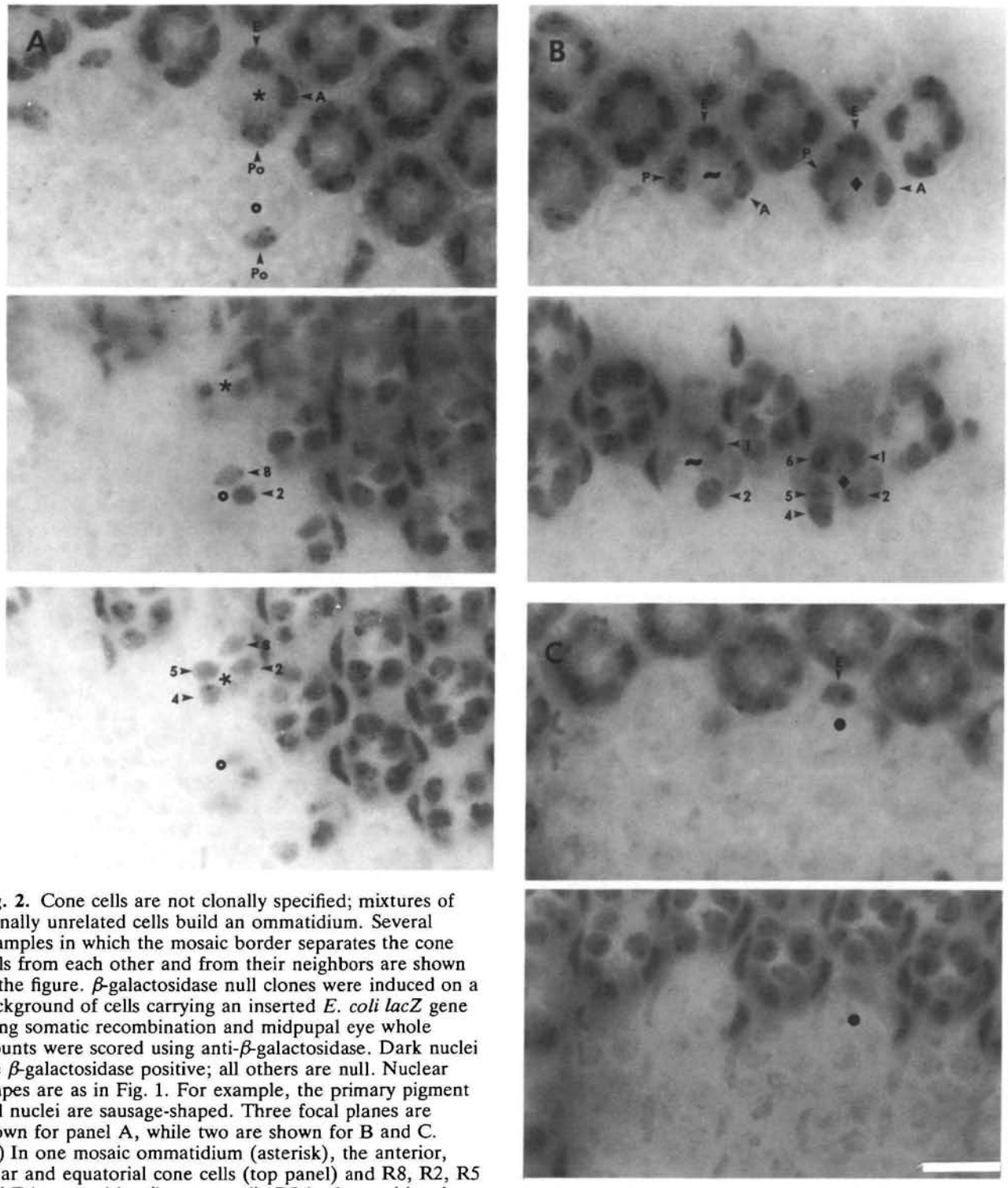

Fig. 2. Cone cells are not clonally specified; mixtures of clonally unrelated cells build an ommatidium. Several examples in which the mosaic border separates the cone cells from each other and from their neighbors are shown in the figure. β-galactosidase null clones were induced on a background of cells carrying an inserted *E. coli lacZ* gene using somatic recombination and midpupal eye whole mounts were scored using anti-β-galactosidase. Dark nuclei are β-galactosidase positive; all others are null. Nuclear shapes are as in Fig. 1. For example, the primary pigment cell nuclei are sausage-shaped. Three focal planes are shown for panel A, while two are shown for B and C. (A) In one mosaic ommatidium (asterisk), the anterior, polar and equatorial cone cells (top panel) and R8, R2, R5 and R4 are positive (lower panel); R3 is also positive, but is out of the focal plane. In an adjacent mosaic ommatidium (open circle), the polar cone cell (top panel) and R2 and R8 (middle panel) are positive for β-galactosidase. All remaining cells are null. These two examples illustrate the non-clonality of the cone cells and the non-clonality of the equatorial cone cell and R7. (B) In a mosaic ommatidium (diamond) the anterior, posterior and equatorial cone cells are β-galactosidase positive (top panel); photoreceptors R8 (out of focal plane), R2, R5, R4, R1 and R6 are β-galactosidase positive (lower panel). In a second mosaic ommatidium (tilde), the anterior, posterior and equatorial cone cells are β-galactosidase positive, (top panel) while only R1 and R2 are positive for β-galactosidase (bottom panel). (C) In a mosaic ommatidium (solid circle), only the equatorial cone cell expresses β-galactosidase (top panel); all photoreceptors are null for β-galactosidase (bottom panel). A, anterior; P, posterior; Po, polar; E, equatorial. Numbers indicate photoreceptor numbers. Bar, 10 μm. Anterior to the right.

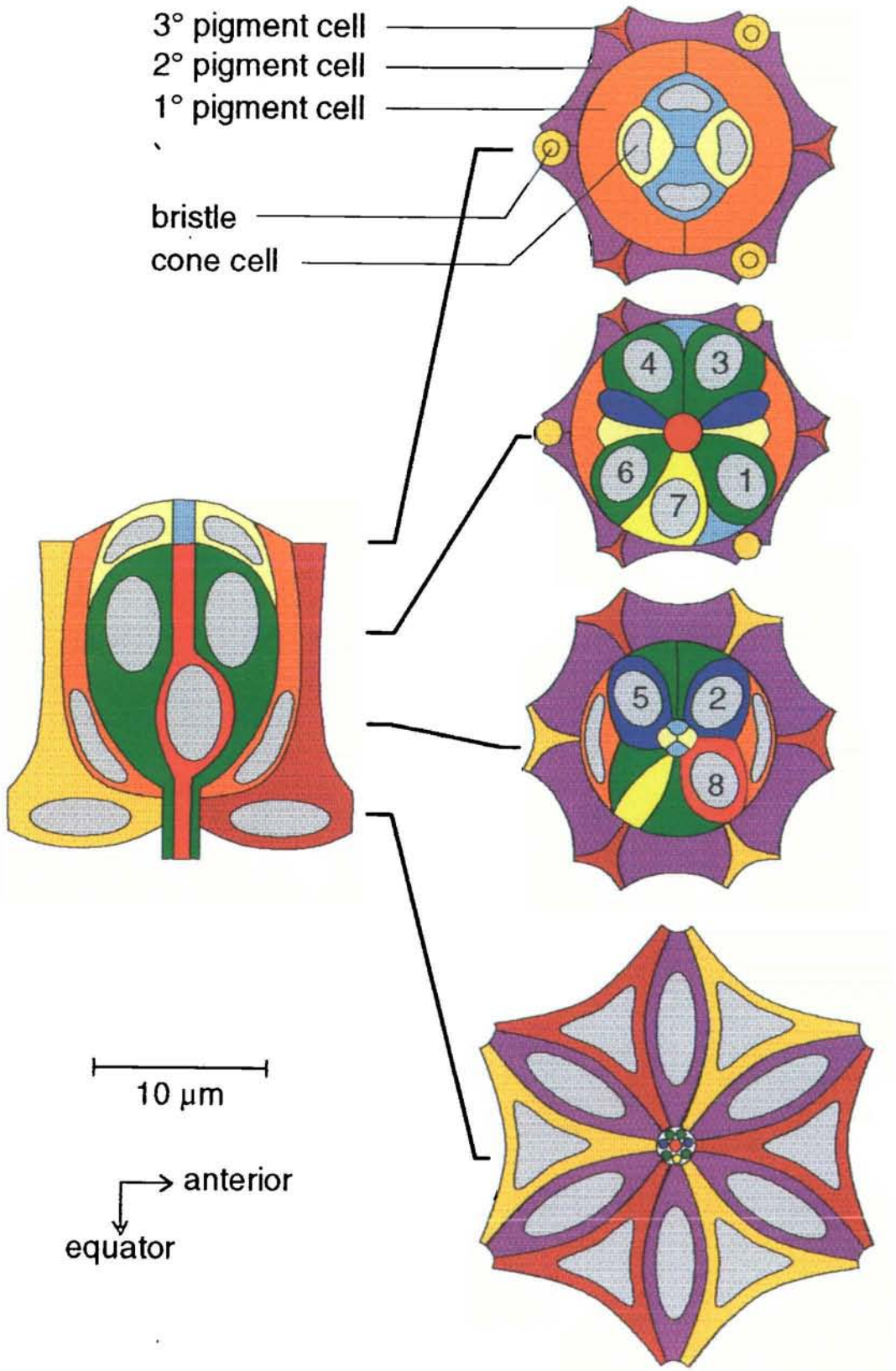

Fig. 1. Schematic 65 h ommatidium. Cellular pattern formation is complete by approximately 65 h at 20°C (33 % of pupal life). Mechanosensory bristle complexes consisting of four cells are indicated by a single cell. The side view is equatorial to the midplane and does not contain the small basal processes of the cone cells seen in the cross sections. Photoreceptors are numbered and nuclei are indicated in gray. For a discussion of retinal cell types see Cagan and Ready (1989*b*).

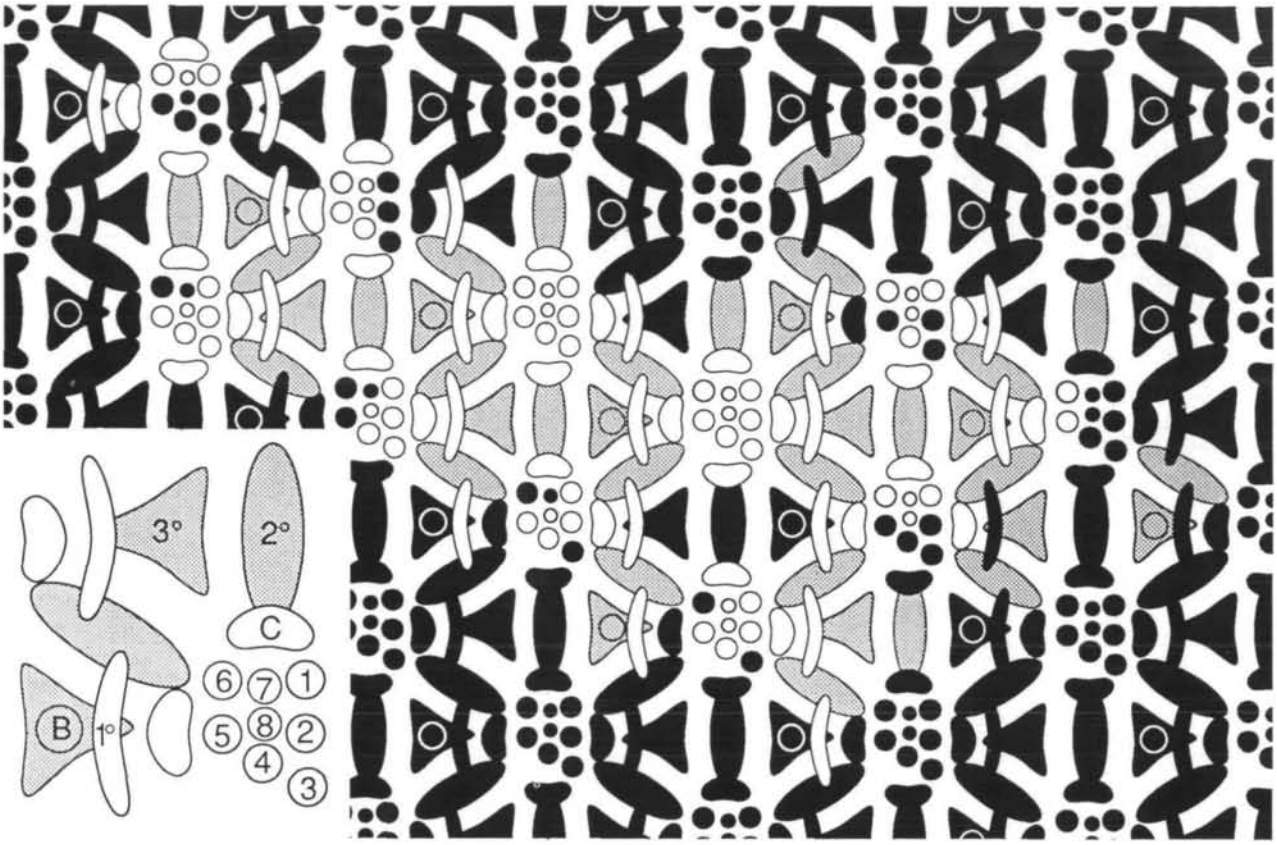

Fig. 3. A β-galactosidase null clone. For clarity of the score sheet, secondary and tertiary pigment cells and bristles are shaded as in the inset. β-galactosidase-positive cells are black. Photoreceptors R1–8 are numbered. C, cone cell; B, bristle; 1°, primary pigment cell; 2°, secondary pigment cell; 3°, tertiary pigment cell. The mosaic contains several examples of clonal separations of the cone cell from each other and their neighbors. Anterior to the right.

Cell contacts and cell death

Specific cell–cell contacts are a hallmark of the eye pattern, and a plausible repository for cell fate determining signals. The determination of whether certain contacts promote survival or death would be greatly facilitated by a marker that would identify moribund cells before they disappear from the apical surface and fragment; once a cell loses its apical contacts it is no longer possible to read who its neighbors were. We have investigated a number of markers reported to be associated with early phases of cell death but none identified dying cells in the eye. Ubiquitin levels have been reported to rise in dying cells (Schwartz *et al.* 1990). Neither polyclonal nor monoclonal anti-ubiquitin antibodies stained dying retinal cells. Similarly, an increase in β-galactosidase was not seen in dying cells in flies containing a polyubiquitin promoter β-galactosidase fusion gene. Increases in acid phosphatase during early stages of cell death have been described in some systems (Lockshin, 1981; Skelton and Bowen, 1987), but application of these protocols to fly eyes did not identify dying cells.

A form of positional bias, perhaps contact-mediated, is suggested by the preferential elimination of cells adjacent to bristle groups. In thin sections, dying cells are frequently encountered next to bristles. Cells about to die present greatly reduced apical profiles in lead sulfide-stained eyes. At 50 h, when cell death is eliminating surplus secondary and tertiary pigment cells, 93 % of the cells with small profiles had bristles as neighbors (Fig. 11E). The remaining 7 % appeared at vertices occupied by a tertiary pigment cell. Although bristles may strongly bias the selection of cells for death, they cannot be the sole determinant since the lattice resolves correctly around the perimeter of the eye, where bristles are absent.

Cell death appears to occur uniformly over the entire eye, rather than sweeping from the back to front, like the morphogenetic furrow, or radiating from the center out, as in the pattern of cell divisions that generates the bristle groups (Cagan and Ready, 1989*b*).

Acridine orange staining parallels the loss of cells from the apical surface

When cells die, they fragment into a variable number of spheres, typically about a dozen. These fragments stain intensely with acridine orange (AO), which is excluded from healthy cells (Spreij, 1971). When pupal eyes were stained with AO at five hour intervals, only scattered AO-stained fragments were found in eyes between 25–40 h (Fig. 7A). At 45 h, most eyes show a dramatic increase in staining, although occasional 45 h eyes have only a few stained fragments. All 50 h eyes are heavily

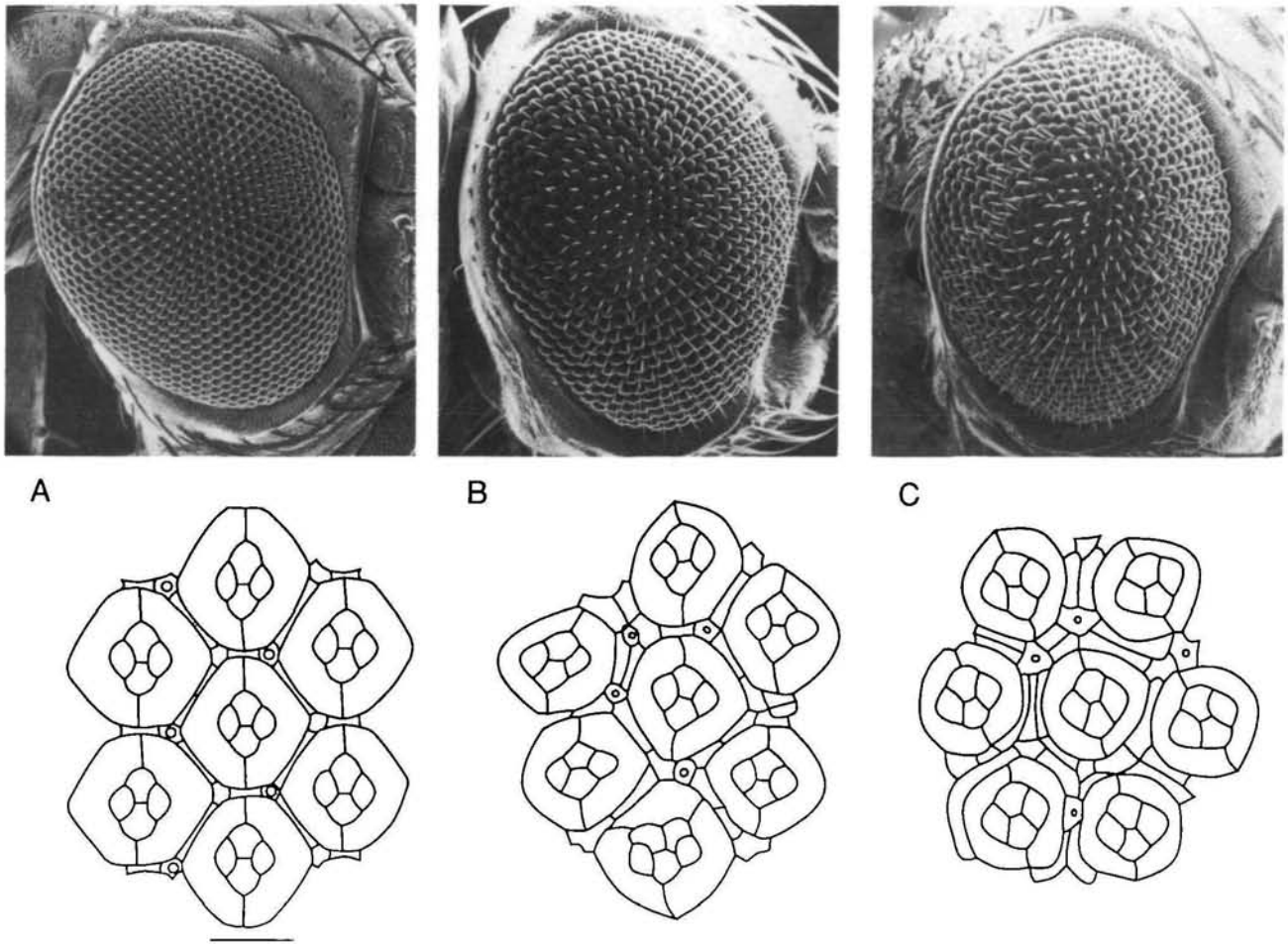

Fig. 4. Scanning electron micrographs (top) and representative fields traced from the apical surfaces of cobalt sulfide-stained midpupal eyes using video microscopy (bottom). (A) Wild type, (B) *echinus* and (C) *roughest*. *ec* is mildly rough with rare 5 cone cell groups and occasional tripled 1° pigment cells; 2° pigment cells are frequently doubled in *ec*. rst^{CT} eyes are rougher; 2° pigment cells are either doubled or tripled in rst^{CT}. Refer to Fig. 1 for cell identities. Bar, 10 μm. Anterior to the right.

stained (Fig. 7B), suggesting a rapid onset of staining around 45 h. Heavy staining persists into 55 h, but is greatly reduced by 60 h (Fig. 7C), and absent by 65 h.

There is a pronounced lag between the time a cell loses its apical foothold, as measured by the cell counts in pupal eyes, and the onset of AO staining. Cell numbers decline steeply between 35 and 40 h whereas AO staining does not begin until 45 h; cell fragments appear to remain selectively permeable for several hours.

Perimeter clusters die midway through pupation

Around the perimeter of the eye is a population of stunted ommatidia that do not persist into adult life (Fig. 8). Virtually every ommatidial row ends in one of these stunted clusters which frequently contain a full complement of photoreceptors, cone cells and primary pigment cells. These perimeter clusters die between 60 and 70 h, as shown by their disappearance from the apical surface of cobalt-sulfide-stained eyes and the ensuing increase of AO-stained fragments. Occasional AO-stained fragments are seen on the perimeter of 60 h eyes and by 65 h this cellular debris is abundant (Fig. 9A). Peripheral staining remains bright through 70 h and, by 75 h, only scattered clusters of AO staining fragments remain. Five hours later, only an occasional pycnotic body is seen on the perimeter. Unlike the dispersed cell death that occurs between 35 and 55 h, death on the perimeter involves elimination of entire ommatidia.

In the retina, the pigment cells that were established in coordination with these stunted ommatidia survive. As a result, the pigment cell lattice extends to the perimeter of the eye rather than fraying on the edge. Perimeter clusters were independently discovered by Hanson (unpublished manuscript) who suggested that they organize the optic cartridges of the underlying optic brain, the lamina, which serve as the innervation targets for ommatidia on the perimeter of the adult eye (Trujillo-Cenóz and Melamed, 1966; Braitenberg, 1967).

Cell death in larval discs

A low level of cell death occurs in third instar larval eye

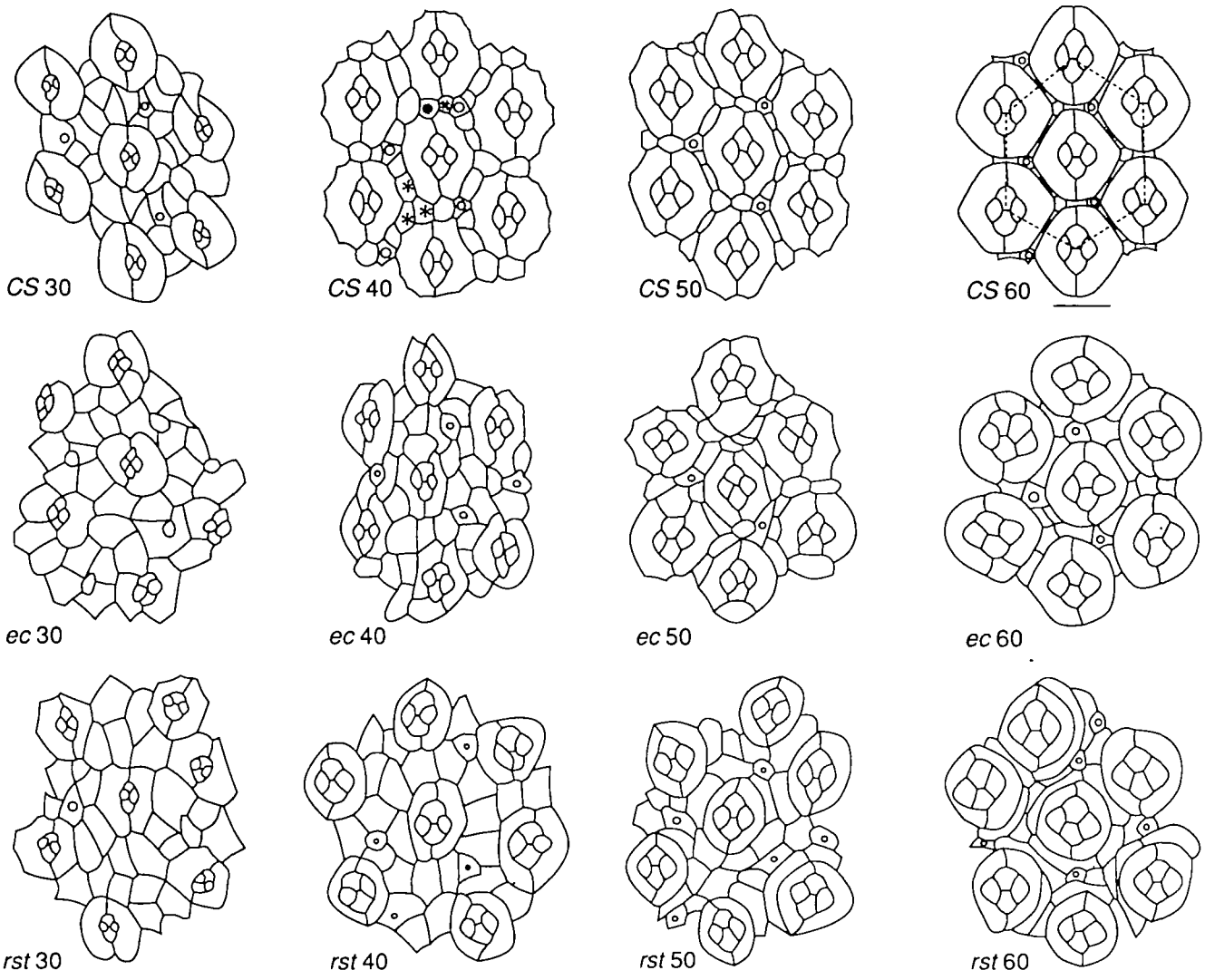

Fig. 5. Pattern formation in normal and mutant pupal eyes. Video microscope tracings of cobalt sulfide-stained pupal eye whole mounts. Refer to Fig. 1 for cell identities. Photoreceptors are not represented on the apical surface of pupal eyes. In wild type, cell death resolves the pigment cell lattice between 35 and 55 h. In *ec* and rst^{CT}, too few cells die and the pigment cell lattice is scrambled. Dashed hexagon in CS60 defines the target area used for cell counts. Bar, 10 μm; anterior to the right.

discs. Using AO staining, we find two significant bands of dead cells, one ahead of the furrow and one near the posterior margin of the eye disc (Fig. 10A). Directly behind the furrow is a zone free of stained fragments, extending approximately 10–12 rows posterior to the furrow. Posterior to this region a variable number of AO-staining dead cells, typically 15–20, are scattered across the disc. As in the pupal eye, there is a lag between cell fragmentation and the onset of AO staining; spherical, refractile cell fragments occur several rows ahead of AO staining. AO and Feulgen stains demonstrate the presence of a second band of death located immediately anterior to the furrow of mature third instar discs in the region of undifferentiated cells. This band of death consists of fragments from approximately 10–20 cells. The significance of this low level of cell death is not known.

Early third instar discs have fewer fragments than late thirds and dying cells do not appear at the posterior of the disc until after about 10 ommatidial rows have formed. Cell death is essentially absent in second larval instar eye discs.

Other investigators have also observed a band of AO-stained fragments anterior to the furrow (Spreij, 1971; Bonini *et al.* 1990). We have not seen the band of death immediately behind the furrow described by Campos-Ortega *et al.* (1979) and Campos-Ortega (1980) using thin and semi-thin sections.

Structural features of cell death

An extensive EM survey suggests all dying cells in pupal eyes follow a common final path. Dying cells present diverse figures, but they can be ordered into a plausible sequence according to the loss of ultrastructural

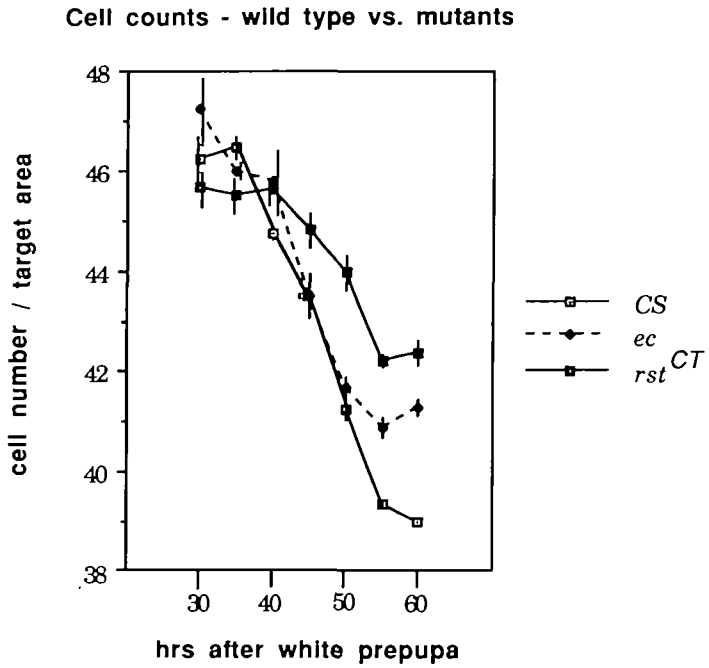

Fig. 6. Cell numbers within a defined target area at 5 h intervals between 30 and 60 h of pupation. Cell death in wild type begins between 35 and 40 h of development and is complete by 60 h. Pattern formation is essentially complete at 55 h; the drop between 55 and 60 h is approximately one third of a cell per target area. Cell death eliminates 7, 5 and 4 cells per target area in wild type, *ec* and rst^{CT}, respectively.

integrity from one to the next (Fig. 11). All fragments from a single cell may not disintegrate in synchrony since, in an isolated spray of debris, presumably from a single cell, the stages of blebs can vary. It is likely that the lifetime of an isolated bleb varies with its size and contents.

Stage 1

Structurally, cell death begins with a collapse of the cell into about 6–12 connected blebs (Fig. 11A). The contents of the blebs vary from those consisting almost entirely of the nucleus to those containing an assortment of organelles. Flanges of the cell's cytoplasm which formerly extended between neighboring cells retreat into the blebs. The apical surface of the dying cell is effaced as neighboring, healthy cells close over it. Nuclear and plasma membranes and organelles appear normal. The cytoplasm undergoes mild condensation and the nucleus begins to round up. The nucleoplasm is not noticeably condensed; its salt and pepper appearance is similar to that of surrounding healthy nuclei. The nucleolus, which is normally heterogeneous and irregular in outline, begins to condense.

A notable early feature of cell death is the loss of microtubules. Microtubules are prominent in healthy cells, and are commonly oriented vertically as well as in loose bundles which lie behind the adherens junctions that join cells at their apical perimeters (Fig. 11F). Microtubules are rare or absent in blebbed cells. A loss of microtubules supports the notion that the disruption of the cytoskeleton is an early event in the structural collapse of the cell (Orrenius *et al.* 1989).

Stage 2

The cytoplasm of the cell becomes increasingly condensed and blebs may disconnect from the nucleus-containing core fragment. The nucleus and nucleolus become dense and spherical, and the nucleolus migrates to the center of the nucleus (Fig. 11B). The nuclear membrane, mitochondria and rough endoplasmic reticulum appear relatively normal. Cell fragments are partially engulfed by neighboring cells; it is likely that they are too large to be entirely engulfed at this stage. Stage two fragments are frequently encountered and probably long-lived.

The relatively normal appearance of organelles and cytoplasm in stage two cells suggests blebs may maintain selective permeability for several hours following the initial collapse of the cell. A common figure in AO-stained eyes is a bright, spherical nucleus with a dense, central nucleolus, typical of late stage two. The lag between the disappearance of cells from the apical surface and the onset of AO staining may reflect the time required for the breakdown of selective permeability.

Stage 3

In the nuclear, core fragment, the nuclear membrane becomes dilated and convoluted. Ribosomes lose their punctate character and become flocculent before being shed from the outer nuclear membrane and rough ER. The nucleus explodes, leaving long strands and whorls of degranulated nuclear membrane mixed in with the cytoplasm of the fragment (Fig. 11C). Mitochondria do not show the dilation seen in necrotic cells. Nucleoli appear more condensed than stage two nucleoli. This highly disrupted stage may coincide with the loss of selective permeability. Non-nuclear fragments condense further as they progress to stage 4.

Stage 4

Cell fragments are highly condensed and appear to be completely engulfed in their final stage of degeneration (Fig. 11D). Nucleoli are still visible as dense cores. Mitochondria are still recognizable and, in some instances, ribosomes remain bound to the ER. Although AO-staining does not persist into 65 h, confocal microscopy shows that engulfed fragments remain in 70 h eyes and are essentially gone by 80 h.

Mutants affecting cell death

Genes participating in cell death are accessible in the eye since disruption of their normal function results in an easily recognizable rough eye. Mutants that fail to eliminate cells from the developing eye cannot assemble the precise cell lattice that gives the eye its regular geometry. Since a variety of developmental defects in addition to a failure of cell death can cause eye roughening, a screen of rough eye mutants is necessary to select candidate cell death mutants. Mid-

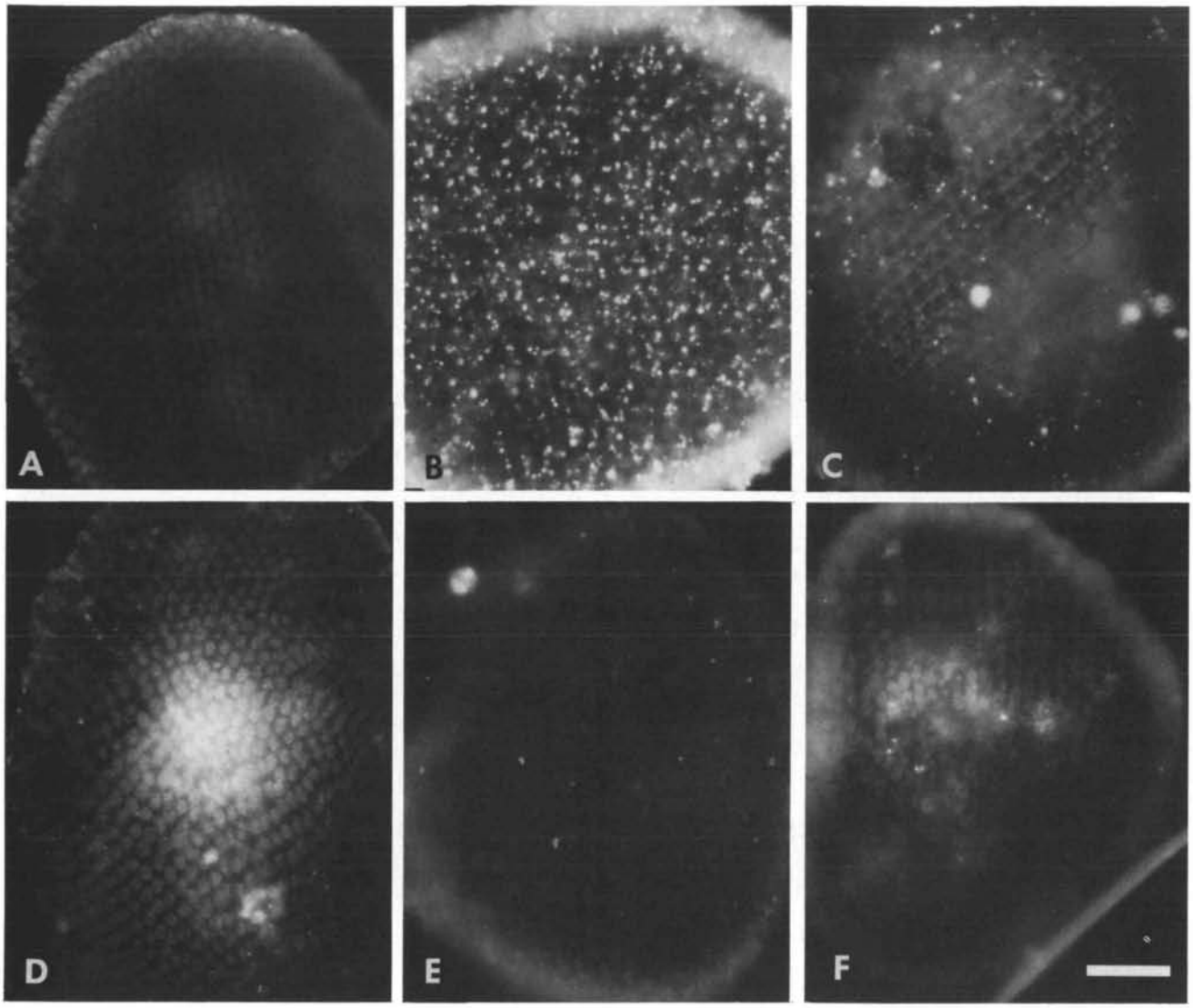

Fig. 7. Cell death in wild type (top) and rst^{CT} (bottom) visualized using AO. Wild-type eyes do not stain at 40 h (A), peak at 50 h (B) and are essentially clear of AO-stained fragments by 60–65 h (C). The burst of AO staining in wild-type eyes is absent in rst^{CT} (D, E and F are 40, 50 and 60 h rst^{CT} eyes, respectively). Bar, 50 μm.

pupal eyes (55 h) were dissected from rough-eyed flies and examined in cobalt-sulfide-stained whole mounts. Since cell death does not operate during the assembly of the photoreceptors, cone cells and primary pigment cells, mutants in which these cells are abnormal were rejected; those with a surplus of interommatidial cells, the population normally winnowed by cell death, were selected for additional study.

In a screen of 9 rough eye mutants two, *echinus* (*ec*) and *roughest*^{CT} (rst^{CT}) were found to have a surplus of interommatidial cells. *ec* eyes are mildly rough relative to rst^{CT} (Fig. 4B and C, respectively). Counts show both mutants have normal numbers of ommatidia.

ec ommatidia have occasional extra cone cells and primary pigment cells (Fig. 4B, lower panel). In *ec*, the extra pigment cells are typically doubled end-to-end, often leading to a jumble of cells at a vertex. A single, spontaneous allele of *ec* exists and has been mapped to 1-5.5.

rst^{CT} eyes have a normal complement of photoreceptors, cones and primaries (Fig. 4C, lower panel). The extra secondaries in rst^{CT} are doubled or tripled side-by-side. An identical phenotype is seen in the second extant *rst* allele, Df(1)rst^2, a spontaneous, male-viable deletion of bands 3C3-5 (Lefevre and Green, 1972). rst^{CT} is an EMS induced allele mapped to 1-2.2 (Lefevre and Green, 1972).

The extra cells in *ec* and rst^{CT} eyes do not stem from an initial overabundance of cells in the retinal epithelium. Cell counts for wild-type and mutant eyes indicate that all begin the phase of cell elimination with an equal number of cells (Fig. 6, t=35 h). The two mutants deviate from wild type as early as 40 h, the time at which cell death begins in the eye (Fig. 6). Final cell

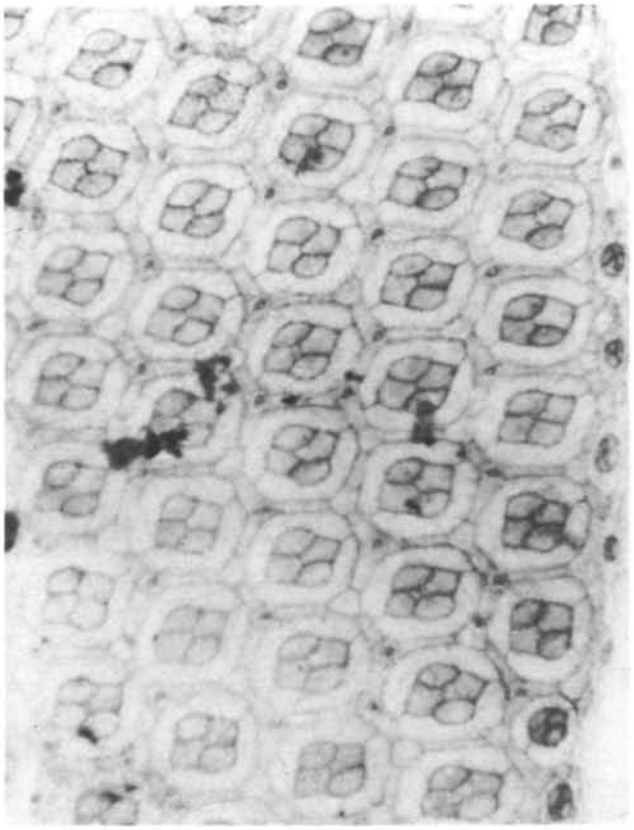

Fig. 8. A population of stunted clusters lies on the perimeter of this cobalt sulfide-stained 60 h wild-type pupal eye. Six stunted clusters lie on the right edge of the figure. Perimeter clusters are also present in rst^{CT} eyes (not shown).

numbers are achieved at the same times in the mutants and wild type.

The surplus cells in *ec* and rst^{CT} are not a result of misregulated cell divisions. In normal eyes, a final wave of cell division follows the morphogenetic furrow (Wolff and Ready, 1991). Mitotic labeling using BUdR injections indicates that patterns of cell division in *ec* and rst^{CT} are normal although the smooth bow-shape pattern of staining seen in wild type is somewhat disrupted in the mutants as a result of the roughening of the pattern (data not shown). Later, inappropriate, cell divisions were also not observed in mutant pupal eyes surveyed for the cell counts.

Pattern formation in roughest *and* echinus

Consistent with the observation that midpupal ommatidia of *ec* and rst^{CT} contain a normal complement of photoreceptors, cone cells and primary pigment cells, early pattern formation in the mutants proceeds approximately correctly. In rst^{CT} furrows, ommatidial rudiments are typically correctly spaced and have proper numbers of cells (Wolff and Ready, 1991). Behind the furrow, as clusters mature and additional photoreceptors are added, rst^{CT} ommatidia pack irregularly, degrading the normal square array of clusters (data not shown). Patterning of cells in *ec* furrows proceeds normally and packing of the ommatidial precursors into the square array is indistinguishable from wild type.

By 30 h into pupal life, the local organization of the cone cells and primaries in rst^{CT} (Fig. 5, rst^{CT} 30) is comparable to wild type but distinct from *ec* (Fig. 5, *ec*30). In both rst^{CT} and wild type, the primaries have occluded extra putative primaries from contacting the cone cell quartet; this process fails occasionally in 30 h *ec* eyes, which later give rise to clusters with extra primary pigment cells. By 40 h, the interommatidial matrix in wild type is more tightly packed than in the mutants so that no side-by-side doublings of secondary or tertiary pigment cells occur. From this point on, cell death drives pattern formation, removing surplus cells from the lattice. Both *ec* and rst^{CT} fail to achieve the level of organization shown by a 40 h wild-type eye.

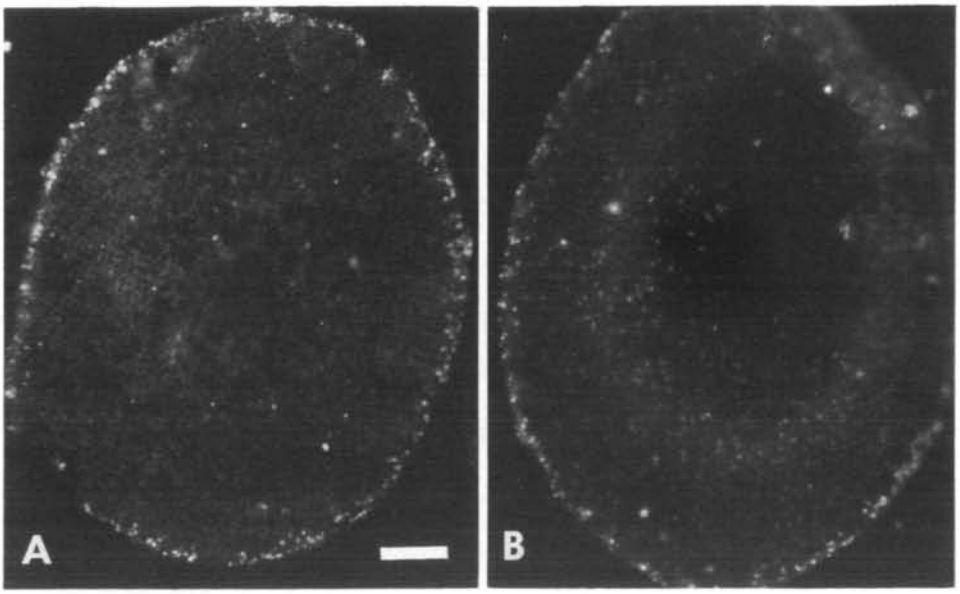

Fig. 9. Perimeter clusters die at about 65 h of pupal life. (A) Wild type. Clusters of dying cells are seen on the edge of this AO stained 70 h wild-type eye. (B) *roughest*. These clusters are also present in rst^{CT} and die on schedule. Bar, 50 μm.

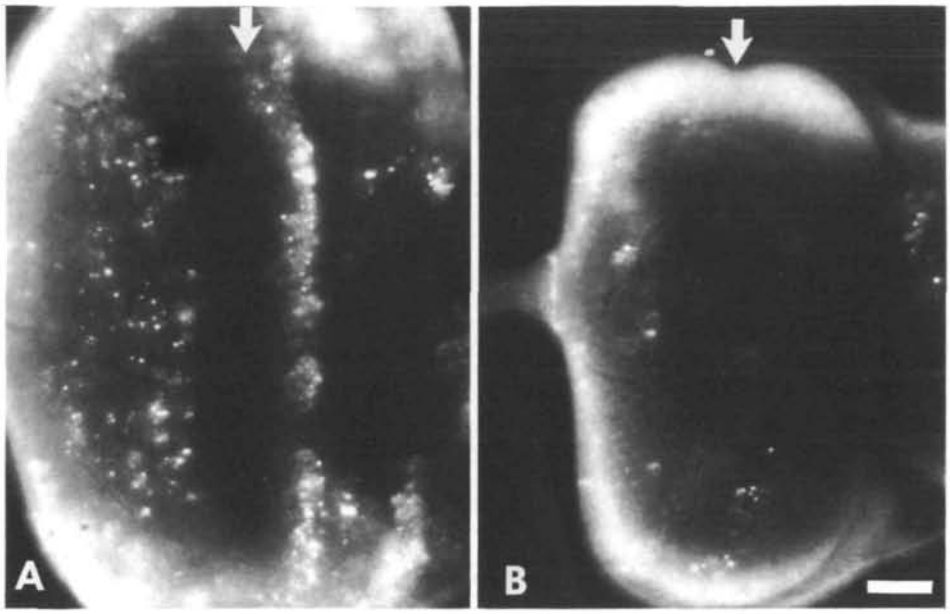

Fig. 10. Cell death in third instar eye discs. (A) Wild type. In this AO stained disc, two bands of dying fragments are seen. Starting about 12 rows posterior to the furrow (arrow) fragments of about 20 cells are seen. A band of dying cells is also seen directly ahead of the furrow. (B) *roughest*. The two bands of death in wild-type eye discs are virtually absent in rst^{CT} discs. Bar, 50 μm; anterior to the right.

This level of organization may be required for the correct assignment of cell death as a fate.

AO staining is absent in roughest

The earliest phase of cell death is not evident in rst^{CT} eye discs (Fig. 10B). Both the pre-furrow and post-furrow bands of death that are prominent in wild-type discs are missing in rst^{CT} eyes, although a few AO-staining fragments are occasionally seen. rst^{CT} does not appear to be eye-specific since death in the antennal disc is also reduced in rst^{CT} as compared to wild type.

The explosion of AO staining seen in 50 to 55 h wild-type eyes is absent in rst^{CT} (Fig. 7, D, E, F). At all times before and after the peak of AO staining, the rst^{CT} pattern of staining is indistinguishable from wild type. Furthermore, engulfed fragments are prominent in 45, 50 and 55 h phalloidin-stained wild-type eyes but absent in rst^{CT} eyes. In an EM survey of 50 h rst^{CT} eyes, dying cells were rarely seen.

Although rst^{CT} is required for interommatidial cell death, it appears to be dispensable for the death of the stunted perimeter clusters, since these are present in the mutant and eliminated on schedule (Fig. 9 B).

The virtual absence of dying cells in rst^{CT} eyes does not agree with the cell counts, which show that about one cell per ommatidium must disappear from the apical surface in the mutant. In normal eyes, a cell's disappearance from the apical surface is a reliable indicator of death; there is an exact correspondence between cells represented on the surface and nuclei lying below. It is possible that in rst^{CT} some cells slip or are forced off the surface, but survive without an apical foothold. A complete reconstruction of a mutant eye might detect such cells, but the scrambled cell patterns of the mutant would make such a reconstruction formidable.

roughest *mosaics*

In mosaic eyes containing homozygous *rst* clones, roughness is coincident with the mutant tissue, suggesting a local action of the gene. In Fig. 12, genetically normal (β-galactosidase positive) cells have assembled into a proper lattice in close proximity to the *rst* clone. Along the border between wild-type and *rst* clones, the pigment cell lattice is strongly disrupted and the potential of mutant cells can be assessed only in rare areas where *rst* cells are incorporated into predominantly wild-type tissue. When small numbers, six or fewer, of *rst* cells project into neighboring, wild-type tissue, the mutant cells can be incorporated into an apparently normal pigment cell lattice. A strict cell autonomy of the gene cannot be determined from these mosaics since a cell's participation in an extended cellular lattice is not a cell autonomous behavior, but rather is dependent on the pattern of surrounding cells.

facet^{strawberry}

rst^2 interacts with another rough eye mutant, $facet^{strawberry}$, a small deletion between 3C5 and 3C7 (Grimwade *et al.* 1985). When in *cis* to fa^{swb}, the nearby rst^2 deletion suppresses eye roughening (Welshons and Welshons, 1985). fa^{swb} is not dosage compensated and the eyes of females are much less rough than male eyes (Welshons and Welshons, 1985).

In about 90% of male fa^{swb} ommatidia, one or both primary pigment cells fail to develop normally and the surrounding pigment cell lattice is disordered (Fig. 13). In cases where a single primary pigment cell forms, it commonly shows a hyperexpansion around the cone cell quartet. When both primaries fail, 4–5 cells can contact the cones, similar to fa^8, in which primary pigment cell development also fails (Cagan and Ready, 1989*a*).

Primary pigment cell development fails only occasionally in female fa^{swb} ommatidia (Fig. 13). Although the pigment cell lattice is imperfect in regions

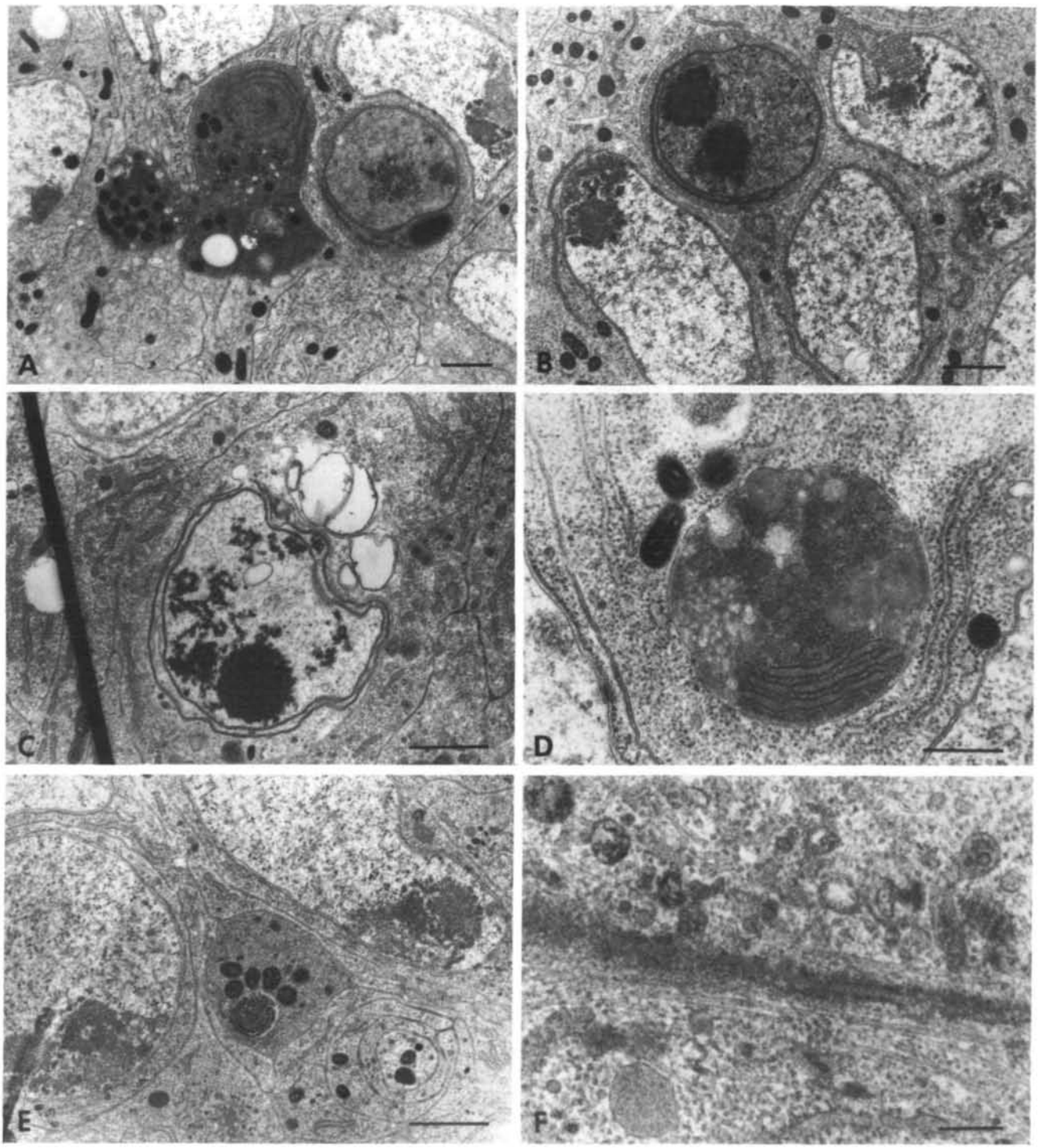

Fig. 11. Dying cells follow a stereotyped sequence of ultrastructural changes. (A) Stage 1; bar, 1 μm. (B) Stage 2; bar, 1 μm. (C) Stage 3; bar, 1 μm. (D) Stage 4; bar, 0.5 μm. (E) bar, 1 μm. (F) bar, 0.25 μm. See text for details.

of apparently normal cones and primaries, cells adjacent to failed primaries are far less ordered.

Discussion

The central questions of cell death in the developing *Drosophila* eye, what informs a cell of its untimely end and how is the sentence executed, remain unanswered. The close description of cell death in normal eyes and the sensitivity of the eye's orderly geometry to mutations perturbing cell death combine to make these questions accessible to the genetic, cellular and molecular methods available in *Drosophila*.

Two distinct regulators of cell death appear to operate during eye development. On the perimeter of

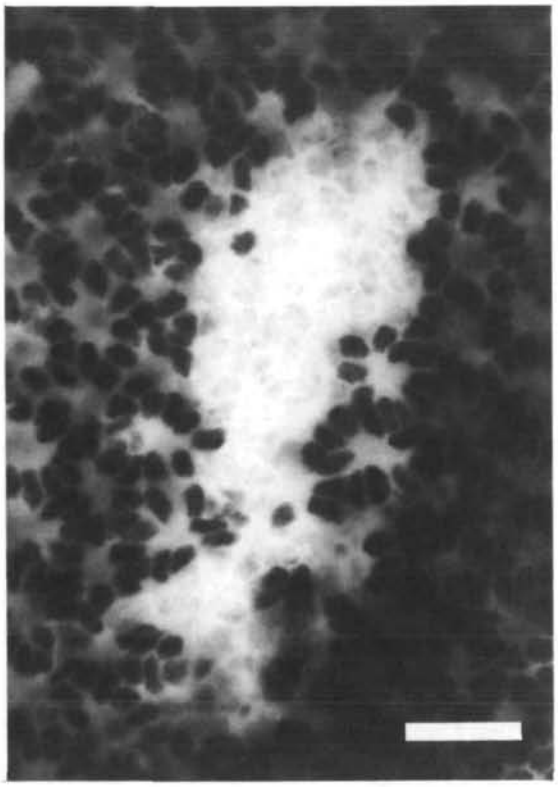

Fig. 12. A pupal eye whole mount showing a clone of homozygous *rst* cells, lacking β-galactosidase activity, on a genetically normal, β-galactosidase-positive background. The floor of the retina is shown. Bar, 15 μm.

the eye, the entire assemblies of differentiated cells that make up the special edge ommatidia die. Except for the photoreceptors, which extend axons and appear grossly normal, cells of these doomed ommatidia never expand to the size and shape appropriate for their cell type, suggesting they are programmed for their fate from an early stage. In contrast, the two to three extra cells per ommatidium that are removed over the expanse of the eye are not distinct from their neighbors. One simple interpretation is that all undetermined cells trapped between ommatidia are equivalent in their potential to survive and that supracellular patterning rules, for example based on combinations of specific cell–cell contacts, determine which cells live and which die. Although perimeter and interommatidial cell death appear the same ultrastructurally, it is premature to conclude that the mechanisms that implement a cell's decision to die are the same for both populations.

Observations using cellular and molecular methods suggest cell death is a directed cell fate requiring an active response by the dying cell (Horvitz *et al.* 1982; Oppenheim *et al.* 1990); dependent cells deprived of their growth factors live longer when the synthesis of new proteins is blocked. One interpretation of these and other results is that cells contain a genetically encoded 'suicide program' whose execution is prevented by access to some form of survival factor. Mutations affecting such a 'suicide' pathway may occur in the *cell death-3* (*ced-3*) and *ced-4* mutants of the nematode, *Caenorhabditis elegans*. In these animals, almost all normally occurring cell deaths are blocked (Ellis and Horvitz, 1986). rst^{CT} does not appear to be an absolute block in a suicide pathway since cell death eliminates perimeter clusters on a normal schedule in these mutants. One possibility is that distinct pathways can trigger cell death, and rst^{CT} is defective in one of these pathways, rather than the suicide program itself.

Dying cells often appear to be the losers in a competition for access to survival-promoting cell contacts (Oppenheim, 1989). Other cell fates in the eye are specified by cell–cell contacts, and it seems reasonable that they may also toll the final fate. The high frequency of cells dying next to bristles suggests bristles make very bad nextdoor neighbors. Whether cell contacts convey explicit instructions to live or die, or only put cells at relative advantage or disadvantage in a competitive environment, is not known. The survival of extra cells in mutant eyes could as easily reflect the flawed transmission of a specific signal as a general relaxation of competition. The occurrence of extra cone cells and primary pigment cells in *ec* eyes raises the intriguing possibility that *ec* may participate in competitive interactions that normally select these cells.

Although cell death may be intrinsically programmed or controlled by local cues such as cell contacts, the

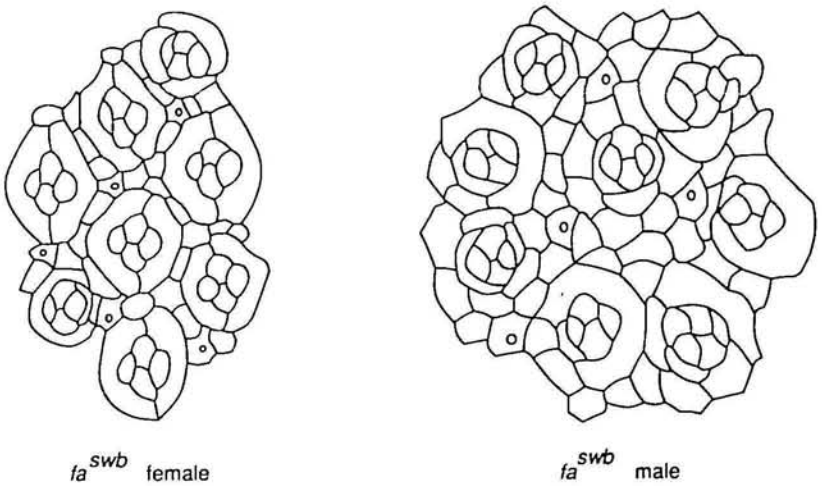

Fig. 13. Midpupal cell patterns of fa^{swb} female and male eyes. In fa^{swb}, normal primary pigment cell development fails. Males show a more frequent primary pigment cell failure and a more extreme disturbance of the pigment cell lattice. Ommatidia containing extra cone cells and primary pigment cells typically overlie monster photoreceptor groups.

roughly synchronous death of cells over large territories is also compatible with a role for diffusible factors in cell death. In *Manduca*, the breakdown of larval muscles just prior to eclosion has been shown to result from decreasing titers of ecdysteroids (Schwartz and Truman, 1983). Significant changes in hormone levels occur during pupal life, about the time of cell death in the eye, and could provide a signal for cells to die or withdraw a growth factor on which cells have become dependent.

Significant pattern changes precede the major phase of cell death in the eye. Between 30 and 35 h after pupation, the cone cells and then the primary pigment cells enlarge and take on their definitive shapes. As primary pigment cells dominate the apical surface, interommatidial cells are increasingly constrained between adjacent ommatidia. A notable common theme in the mutants described here, *echinus*, *roughest* and *facet*^{strawberry}, as well as in *facet*^{glossy} (Cagan and Ready, 1989*a*), is the failure of primary pigment cells to develop normally. In these eyes, interommatidial cells are less constrained and fewer cells die. This defect may prevent the formation of contacts required for later sorting and could remove an important impetus for cell elimination.

Cell death has been considered a directed cell fate, and in the fly eye cell death is the final fate to be specified. After the tight burst of cell death that completes pattern formation, each cell occupies its definitive position and the generation of specialized, cell-type-specific products accelerates greatly. The quantitation of cell death reported here agrees with the lower resolution survey of Cagan and Ready (1989*a*). It does not, however, support the division of cell death into an early (20–36 h) and late (36–100 h) phase as reported in Cagan and Ready (1989*b*). This discrepancy is likely to be a result of different methods used for quantitating dead cells in the previous work. Feulgen staining, which was was used to identify the pycnotic nuclei of dead and dying cells is complicated by the dispersal of cells into variable number of fragments and the high background of stained normal nuclei.

The stereotyped sequence of events in wild-type cell death broadly parallels descriptions in *Drosophila* mutants (Fristrom, 1969) as well as other systems (Wyllie, 1981; Robertson and Thomson, 1982; Kerr *et al.* 1987), but there are important differences. The explosion of the nucleus in stage 3, for example, resembles an event in necrosis, cell death caused by injury, rather than the progressive condensation usually reported in programmed cell death. Also, condensation of the heterochromatin against the nuclear membrane, or margination, reported as the earliest sign of vertebrate cell death (Bowen and Lockshin, 1981), does not occur during cell death in the fly eye. Details of the structural collapse of a dying cell may vary depending on the tissue type (Clarke, 1990).

We thank Dr S. Muller and Dr V. Fried for generously supplying anti-ubiquitin antibodies. Polyubiquitin promoter–*lacZ* constructs were provided by Dr J. Lis. Dr Seth Blair provided helpful staining protocols. We thank Dr Nancy Bonini for useful comments on the manuscript. Dr Chris Sahley provided advice on statistical methods. This work was supported by USPHS grant no. RO1 AG09302.

References

Baumann, O. and Walz, B. (1989). Topography of Ca^{++}-sequestering endoplasmic reticulum in photoreceptors and pigmented glial cells in the compound eye of the honeybee drone. *Cell and Tissue Research* **255**, 511–522.

Bellen, H., O'Kane, C. J., Wilson, C., Grossniklaus, U., Kurth-Pearson, R. and Gehring, W. J. (1989). P-element-mediated enhancer detection: A versatile method to study development in *Drosophila*. *Genes Dev.* **3**, 1288–1300.

Bier, E., Vaessin, H., Shephard, S., Lee, K., McCall, K., Barbel, S., Ackerman, R., Carretto, R., Uemura, T., Grell, E. H., Jan, L. Y. and Jan, Y. N. (1989). Searching for pattern and mutations in the *Drosophila* genome with a P-*lacZ* vector. *Genes Dev.* **3**, 1273–1287.

Blair, S. (1991). Gene expression and the development of anterior and posterior lineage compartments in the imaginal wing disc of *Drosophila*. (submitted)

Bonini, N., Leiserson, W. and Benzer, S. (1990). A mutation in compound eye development of *Drosophila* that results in cell death rather than differentiation. *J. cell. Biochem.* **14E**, 502.

Bowen, I. D. and Bowen, S. M. (1990). *Programmed Cell Death in Tumors and Tissues*. Chapman and Hall, London.

Bowen, I. D. and Lockshin, R. A. (1981). *Cell Death in Biology and Pathology*. Chapman and Hall, London.

Bowen, I. D. and Ryder, T. A. (1974). Cell autolysis and deletion in the planarian *Polycelis tenuis* Iijima. *Cell and Tissue Research* **154**, 265–274.

Braitenberg, V. (1967). Patterns of projection in the visual system of the fly. I. Retinal-lamina projections. *Expl Brain Res.* **3**, 271–298.

Cagan, R. L. and Ready, D. F. (1989*a*). *Notch* is required for successive cell decisions in the developing *Drosophila* retina. *Genes Dev.* **3**, 1099–1112.

Cagan, R. L. and Ready, D. F. (1989*b*). The emergence of order in the *Drosophila* pupal retina. *Devl Biol.* **136**, 346–362.

Campos-Ortega, J. A. (1980). On compound eye development in *Drosophila melanogaster*. In *Current Topics in Developmental Biology*, vol. 15 (ed. A. A. Moscona and A. Monroy), pp. 347–371. Academic press, New York.

Campos-Ortega, J. A., Jurgens, G. and Hofbauer, A. (1979). Cell clones and pattern formation: Studies on *sevenless*, a mutant of *Drosophila melanogaster*. *Wilhelm Roux's Arch. devl Biol.* **186**, 27–50.

Chayen, J., Bitensky, L., Butcher, R. and Poulter, L. (1969). *A Guide to Practical Histochemistry*. J. B. Lippencott, Philadelphia.

Clarke, P. G. H. (1990). Developmental cell death: morphological diversity and multiple mechanisms. *Anat. Embryol.* **181**, 195–213.

Ellis, H. M. and Horvitz, H. R. (1986). Genetic control of programmed cell death in the nematode *C. elegans*. *Cell* **44**, 817–829.

Fristom, D. (1969). Cellular degeneration in the production of some mutant phenotypes in *Drosophila melanogaster*. *Molec. gen. Genetics* **103**, 363–379.

Grimwade, B. G., Muskavitch, M. A. T., Welshons, W. J., Yedvobnick, B. and Artavanis-Tsakonas, S. (1985). Molecular genetics of the Notch locus in *Drosophila melanogaster*. *Devl Biol.* **107**, 503–519.

Horvitz, H. R., Ellis, H. M. and Sternberg, P. W. (1982). *Neurosci. Comment.* **1**, 56.

Kerr, J. F. R., Searle, J., Harmon, B. V. and Bishop, C. V. (1987). Apoptosis. In *Perspectives on Mammalian Cell Death* (ed. C. S. Potten), pp. 93–128. Oxford, New York.

Lawrence, P. A. and Green, S. M. (1979). Cell lineage in the developing retina of *Drosophila*. *Devl Biol.* **71**, 142–152.

Lefevre, G. and Green, M. M. (1972). Genetic duplication in the

white-split interval of the X chromosome in *Drosophila melanogaster*. *Chromosoma* **36**, 391–412.

LINDSLEY, D. L. AND GRELL, E. H. (1968). *Genetic Variations of* Drosophila melanogaster. Carnegie Inst publ no. 627, Washington DC.

LOCKE, M. AND HUIE, P. (1981). Epidermal feet in pupal segment morphogenesis. *Tissue and Cell* **13**, 787–803.

LOCKSHIN, R. A. (1981). Cell death in metamorphosis. In *Cell Death in Biology and Pathology* (eds. I. D. Bowen and R. A. Lockshin), pp. 79–121. Chapman and Hall, London and New York.

MELAMED, J. AND TRUJILLO-CENOZ, O. (1975). The fine structure of the eye imaginal disc in *muscoid* flies. *J. Ultrastruct. Res.* **51**, 79–93.

MULLER, S., BRIAND, J. AND VAN REGENMORTEL, M. H. V. (1988). Presence of antibodies to ubiquitin during the autoimmune response associated with systemic lupus erythematosus. *Proc. natn. Acad. Sci. U.S.A.* **85**, 8176–8180.

O'KANE, C. AND GEHRING, W. J. (1987). Detection *in situ* of genomic regulatory elements in *Drosophila*. *Proc. natn. Acad. Sci. U.S.A.* **84**, 9123–9127.

OPPENHEIM, R. W. (1989). The neurotrophic theory and naturally occurring motoneuron death. *Trends Neurosci.* **12**, 252–255.

OPPENHEIM, R. W., PREVETTE, D., TYTELL, M. AND HOMMA, S. (1990). Naturally occurring and induced neuronal death in the chick embryo *in vivo* requires protein and RNA synthesis: evidence for the role of cell death genes. *Devl Biol.* **138**, 104–113.

ORRENIUS, S., MCCONKEY, D. J., BELLOMO, G. AND NICOTERA, P. (1989). Role of Ca^{2+} in toxic cell killing. *Trends Pharm. Sci.* **10**, 281–285.

READY, D. F., HANSON, T. E. AND BENZER, S. (1976). Development of the *Drosophila* retina, a neurocrystalline lattice. *Devl Biol.* **53**, 217–240.

ROBERTSON, A. M. G. AND THOMSON, J. N. (1982). Morphology of programmed cell death in the ventral nerve cord of *Caenorhabditis elegans* larvae. *J. Embryol. exp. Morph.* **67**, 89–100.

SCHWARTZ, L. M., MYER, A., KOSZ, L., ENGELSTEIN, M. AND MAIER, C. (1990). Activation of polyubiquitin gene expression during developmentally programmed cell death. *Neuron* **5**, 411–419.

SCHWARTZ, L. M. AND TRUMAN, J. W. (1983). Hormonal control of rates of metamorphic development in tobacco hornworm *Manduca sexta*. *Devl Biol.* **99**, 103–114.

SKELTON, J. K. AND BOWEN, I. D. (1987). The cytochemical localisation and backscattered electron imaging of acid phosphatase and cell death in the midgut of developing *Calliphora vomitoria* larvae. *Epithelia* **1**, 213–223.

SPREIJ, TH. E. (1971). Cell death during the development of the imaginal discs of *Calliphora erythrocephala*. *Netherlands J. Zool.* **21**, 221–264.

TRUJILLO-CENOZ, O. AND MELAMED, J. (1966). Compound eye of Dipterans: anatomical basis for integration – an electron microscope study. *J. Ultrastruct. Res.* **16**, 395–398.

WELSHONS, W. J. AND WELSHONS, H. J. (1985). Suppression of the *facet-strawberry* position effect in *Drosophila* by lesions adjacent to Notch. *Genetics* **110**, 465–477.

WOLFF, T. AND READY, D. F. (1991). The beginning of pattern formation in the *Drosophila* compound eye: the morphogenetic furrow and the second mitotic wave. *Develepment* **113**, 841–850.

WYLLIE, A. H. (1981). Cell death: a new classification separating apoptosis from necrosis. In *Cell Death in Biology and Pathology* (eds. I. D. Bowen and R. A. Lockshin), pp. 9–34. Chapman and Hall, New York.

(Accepted 29 July 1991)